Deliverable D2.4

Report on reduced order models for implementation in DILAFACT

Funded by the European Union. Views and opinions expressed are however those of the author(s) only and do not necessarily reflect those of the European Union. Neither the European Union nor the granting authority can be held responsible for them.

Action number: #101138859

Action Acronym: DILAPRO
Action Name: Digital Laser Production

Deliverable Due date: 30/06/2025
Deliverable hand-in date: 31/07/2025

Revision	Date	Author/Organisation	Description
Draft_1	28/07/2025	Sankhya Mohanty (DTU)	Initial version
Draft_2	30/07/2025	Christina Moeslund Zeuthen (DTI)	Edited
Final	31/07/2025	Sankhya Mohanty (DTU)	Upload version

Executive Summary

This report describes the reduced order models (ROM) developed in WP2 of DILAPRO with a goal of implementation within the DILAFACT platform. This report is structured as an accessible report presenting the most relevant codes or software tools that have been identified or developed to meet the modelling requirements of DILAPRO.

The report first introduces the goal of the activity and how the report should be read. Next, the report highlights selected reduced order modelling tools already identified in D2.1, and their deployment readiness status for DILAFACT. Then the report showcases new reduced order modelling tools developed within DILAPRO project.

The new ROMs contain models based on Gaussian Process modelling, models based on deep learning methods as well as hybrid models that combine statistical data with reduced simulations. In the case of Gaussian process methods, ROMs for predicting porosity during laser welding and ROMs for single track process window identification have been described. For ROMs using deep learning methods, generative AI tools for surface topography prediction were first described followed by tools for advanced microstructure segmentation of low-contrast images. Finally, the hybrid ROM technique is described for a case involving powder bed fusion (PBF) of polymer components, especially highlighting its future adaptability to metal PBF in DILAPRO production lines.

The report concludes with a short summary and outlook on activities planned in WP7 where DILAFACT will be developed and assembled. The report will thus form the basis for further reduced order model development work within DILAPRO and will feed into WP7 focusing on integrating the modelling tools into the DILAFACT solution.

List of Abbreviations

AM	Additive Manufacturing
CNN	Convolutional Neural Network
CT	Computed Tomography
DT	Digital Twin
DED	Directed Energy Deposition
EM	Expectation-Maximization
GMM	Gaussian Mixture Models
GP	Gaussian Process
IoU	Intersection-over-Union
MAE	Mean Absolute Error
ML	Machine Learning
PBF	Powder Bed Fusion
POD	Proper Orthogonal Decomposition
RBM	Reduced Basis Methods
ResUNet	Residual UNet
RMSE	Root Mean Square Error
ROM	Reduced Order Modelling
SEM	Scanning Electron Microscopy
XCT	X-ray Computed Tomography

List of Figures

1. Introduction

The primary goal of DILAPRO is to enhance the adoption and effectiveness of laser-based production technology. This will be accomplished through the development of two software tools: DILAFACT for production planning and DILACERT for part certification. Establishing digital twins of the production processes for the selected materials of DILAPRO is a crucial step towards achieving this goal.

Digital twins (DT) of the laser-based processing can be set up following both multiphysics modelling based workflows as well as data-based (machine learning (ML) or statistical modelling) workflows. Since laser-based processes involve complex thermal, mechanical, and microstructural evolution phenomena, multi-physics simulations are often deployed to analyze them. High-fidelity finite element or computational fluid dynamics models can provide accurate predictions yet often require prohibitively long computational times. Reduced order modelling (ROM) methods address this challenge by constructing low-dimensional representations of the system's behaviour, significantly accelerating simulation while retaining essential accuracy.

Reduced order models distil the dominant features of a high-dimensional system into a smaller set of basis functions or surrogate mappings. This compression enables near real-time predictions, design optimization loops, and uncertainty quantification in laser-based manufacturing workflows. As the industry shifts toward digital twins and closed-loop control, ROM strategies become indispensable for integrating simulation-driven insights into process monitoring and adaptive control.

Proper orthogonal decomposition, reduced basis methods, and surrogate modeling form the core of ROM techniques. Each approach identifies patterns or approximations that capture system variability with minimal computational overhead. Proper Orthogonal Decomposition (POD) derives orthogonal modes from snapshot data (e.g., temperature fields over time) representing the dominant energy-containing 'structures' in the system, and subsequently project the governing equations onto this mode space yielding a drastically reduced system of ordinary differential equations. Reduced Basis Methods (RBMs) are based on parameterized simulations, and build a low-dimensional simulation space adaptively. Subsequently, Greedy algorithms select the most informative solution snapshots across the simulated parameter ranges, ensuring error bounds are minimized. Surrogate Models—such as polynomial chaos expansions, neural networks, or Kriging/Gaussian Process —map input parameters directly to output responses. Though they do not solve governing equations, they excel at rapid evaluation across the parameter domain.

This report will focus on ROMs developed within DILAPRO based on Surrogate Modelling techniques primarily and will highlight corresponding models developed through Gaussian Process Regression and Machine Learning methods. First, the report will reiterate some ROM tools already identified in D2.1 and comment on their deployment readiness status. Next, the report will showcase five ROMs created within DILAPRO and provide example results from their deployment. The report concludes with a discussion on the future implementation of the reduced models within DILAFACT, the potential for further model generation based on WP3 activities and the corresponding activities required within WP7 where tools developed in WP2 will be assembled into DILAFACT.

(Please note that unforeseen personnel changes occurred 1 month before submission of this deliverable, in addition to knock-on delays from characterization activities. Consequently, it was agreed with the PO that the report will be submitted with 1-month delay and will contain all functioning ROMs available at that point.)

2. Deployment of prior identified ROM tools

Deliverable 2.1 on "Multi-scale multiphysics simulation framework with hierarchical modelling workflows for selected material" already identified several potential reduced order modelling tools that could be deployed within DILAFACT upon code modification and data update. A short update on their deployment readiness status follows:

2.1 MeltpoolNet ROM

This ROM tool focused on prediction of melt pool characteristics (dimensions and quality) from the build parameters for Laser Power Bed Fusion (LPBF) and Direct Energy Deposition (DED) using Machine learning methods. The tool is trained on literature data sets for laser PBF and DED, with over 2000 datapoints covering multiple materials, such as Ti6Al4V, Ti45-Al, K403 superalloy, IN625, TiC/IN718, IN718, IN738LC, Hastelloy X, Invar36, AlSi10Mg, SS304L, SS316L, SS17-4PH and Cu. The documented process parameters for the model correspond to Power, Velocity, powder flowrate, layer thickness, beam diameter and hatch spacing. The material parameters correspond to the absorption coefficient, density, thermal conductivity, melting temperature, and the elemental composition. The process outputs used for model generation were the depth of meltpool, width of meltpool, length of meltpool, meltpool quality (i.e. lack of fusion, balling, keyhole or desirable), occurrence of spatter and porosity/relative density. The dataset was sparse i.e. process outputs were recorded for each process parameter and material parameter combination.

Multiple pre-trained models were available based on Random Forest, Gaussian Process Regression, Support Vector Machine, Ridge, and Lasso Regression, Gradient boosting trees and Neural Networks. The pre-trained models were verified, the prediction quality was validated for selected DILAPRO process parameter settings, and retraining of models using the original dataset was also performed. The ROM is ready for fine-tuning using the process parameter sets from different DILAPRO production lines, prior to deployment within DILAFACT.

2.2 Differentiable Simulation for Additive Manufacturing ROM

This ROM tool corresponded to a differentiable physics-based thermal simulation code for DED process, also incorporating gradient-based methods for optimizing the process. The tool allows for identification of process parameter setting during the production to achieve a targeted temperature history at specific locations in the produced part. Within DILAFACT, this tool could be deployed to ensure process routes identified through physical simulations (see D2.3 for details on physical simulations) can be recreated during production.

The tool needs to be calibrated for the DED production lines to ensure correct baseline temperature predictions before it can be deployed for process planning. The current tool requires creation of LS-DYNA mesh files and *.crs toolpath files, which need to be generated according to the calibration part. Thus further code development is required to allow for generation of the mesh using open-source finite element software.

2.3 Density_SLM ROM

This ROM tool focused on prediction of the relative density of SS 316L parts produced via PBF. The tool considers PBF process parameters such as laser power, scanning speed, layer thickness, hatch spacing, and powder size. The experimental dataset has 112 data points and was collected from literature spanning PBF machines from different manufacturers. Three statistical metrics—Root Mean Square Error (RMSE), Mean Absolute Error (MAE), and the Coefficient of Determination (R^2)—were combined into an Index of Merit to evaluate and compare the model accuracy. Cross-validation was applied to minimize overfitting and ensure robustness.

The tool is complementary to the machine learning models developed in D3.3, as it considers machines from different manufacturers but does not consider any process monitoring data. The models need to be fine-tuned with relative density datasets from the different DILAPRO production lines before deployment within DILAFACT. In such case, this ROM can predict the expected nominal relative density for selected parameter set, while the advanced models from D3.3 can predict the achieved relative density based on additional process monitoring data.

3. New reduced order modelling tools

Reduced order modelling tools in DILAFACT plan to address the various phenomena occurring at the different length scales of the involved laser processes. Thus, within DILAPRO, multiple ROM tools are developed and/or improved for analysis at the microstructure-scale, the meso-scale (single track and single layer scale) as well as the macro-scale (component scale). Correspondingly, several test specimens have been manufactured to enable extraction, calibration and validation of these ROMs, ranging from single-track and single-layer experiments to cm-scale artefacts to full validation components (e.g. see Figure 1). The combination of the data from these dedicated experiments with the datasets obtained within literature, have allowed a variety of ROM tools to be developed for performing hierarchical modelling of components in laser-based manufacturing. These tools are broadly classified into three categories:

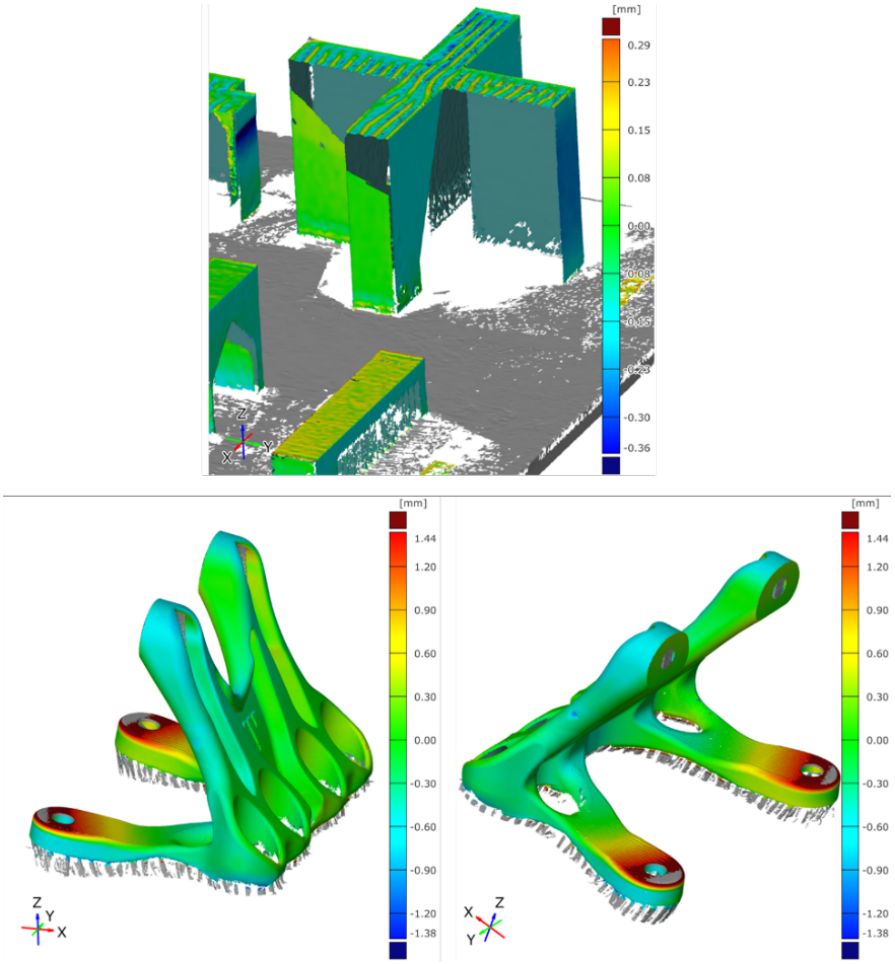

Figure 1 (Top) Calibration part printed for extracting the reduced order assumed strain model, and (bottom) deformation measurement of DILAPRO use-case component printed with same process parameter settings.

3.1 Gaussian Process based ROM

Gaussian Process Models for Laser Manufacturing

Conventional process window exploration involves fabricating and inspecting dozens of single-track specimens—each at a distinct process parameter settings— and often requiring high-resolution microscopy or X-ray computed tomography for subsequent analysis. This empirical approach is both labor- and time-intensive, especially when extended to multiple alloys or novel powder formulations. A data-driven surrogate that interpolates melt-pool behavior between measured points can drastically reduce the required experiments and pinpoint robust operating regions. Gaussian Process (GP) regression offers a flexible, nonparametric surrogate modeling technique well-suited for capturing the involved complex, nonlinear relationships in laser based manufacturing.

Gaussian Process regression treats the unknown function mapping (of process parameters such as power and velocity) to different melt-pool metrics (e.g., depth or width) as a draw from a multivariate normal distribution, conditioned on the training data. The model consequently yields both a predictive mean as well as the variance, allowing users to identify process windows that satisfy target melt-pool criteria with quantified confidence as well as regions of high uncertainty within the process parameter space — the latter being prime candidates for additional experiments. In practice, Gaussian Processes define a distribution over functions, fully specified by a mean function and a covariance kernel. Given training data of input–output pairs, GP regression infers the posterior distribution at new inputs, providing both predictions and uncertainty estimates.

Establishing GP models involves selection of an appropriate kernel and subsequently tuning the hyperparameters (i.e. the different coefficients within the GP) for achieving targeted accuracy. Common kernels include squared exponential, Matérn, and rational quadratic kernel, each controlling smoothness and correlation length scales. The hyperparameter tuning is usually performed using Maximum likelihood or Bayesian approaches.

Gaussian Process Models for porosity prediction during laser welding

This ROM developed within DILAPRO aims to enable rapid prediction of expected porosity for a selected set of laser welding parameters, namely the laser power, the velocity, the laser diameter and the defocus condition (i.e. location of focus position with respect to the surface). The dataset for this work was extracted from a recent study on Al 5754 alloy by Meng et al (Meng et al 2025), which aimed to develop deep learning models using the same. The dataset can be downloaded from https://ars.els-cdn.com/content/image/1-s2.0-S1359645425000333-mmc1.docx . Figure 2 below shows the typical results achieved during

the design of experiments established following a Latin Hypercube Sampling, and the image analysis algorithm based estimation of porosity.

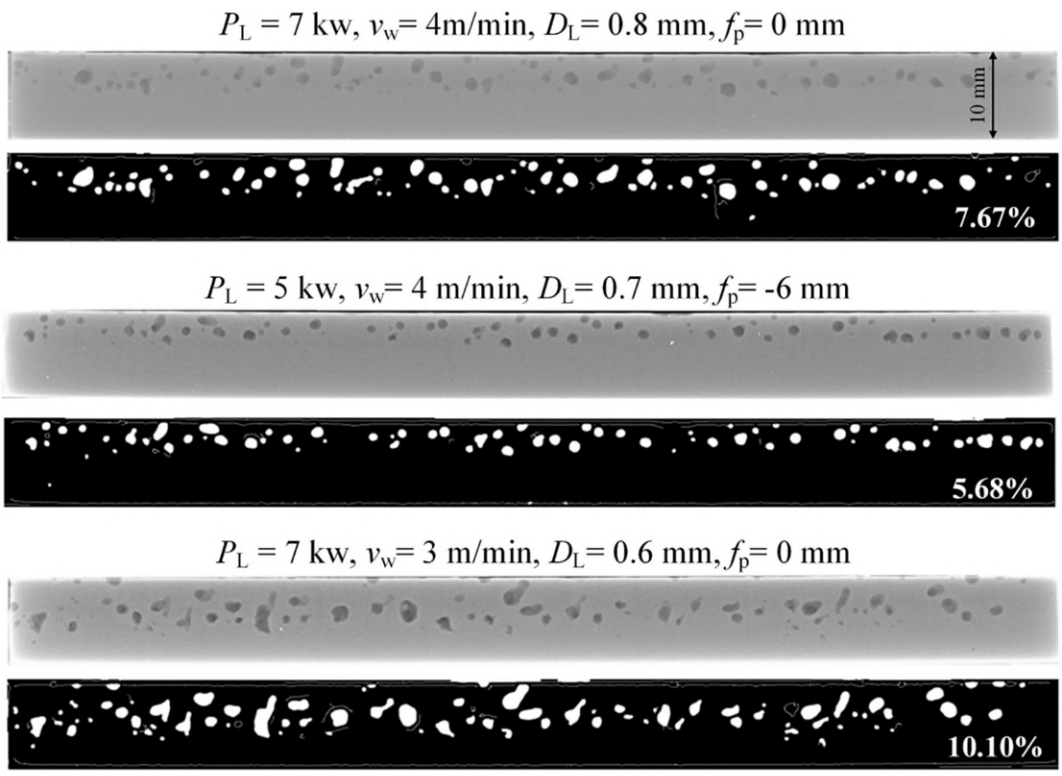

Figure 2 Microscopy images and segmented images for identifying porosity generated during laser welding with different process parameters. The process parameter combinations are shown above the corresponding microscopy images.

Using the GPy modelling tool identified in D2.1, the dataset was used to train a single component Gaussian Process model. Subsequently the developed GP ROM was deployed through a Streamlit app (purely Python-based code) currently hosted at https://laserweld.streamlit.app/ . The developed GP ROM and the corresponding Streamlit app is a demonstrator for the types of ROM-based tools that will used within DILAFACT (for the different laser processing methods). Using the app, users can select different parameter settings for laser power, welding speed, laser diameter, and focus point, and accordingly receive predicted porosity values along with the associated prediction uncertainty (standard deviation). Figure 3 shows a screen-capture image of the Streamlit app.

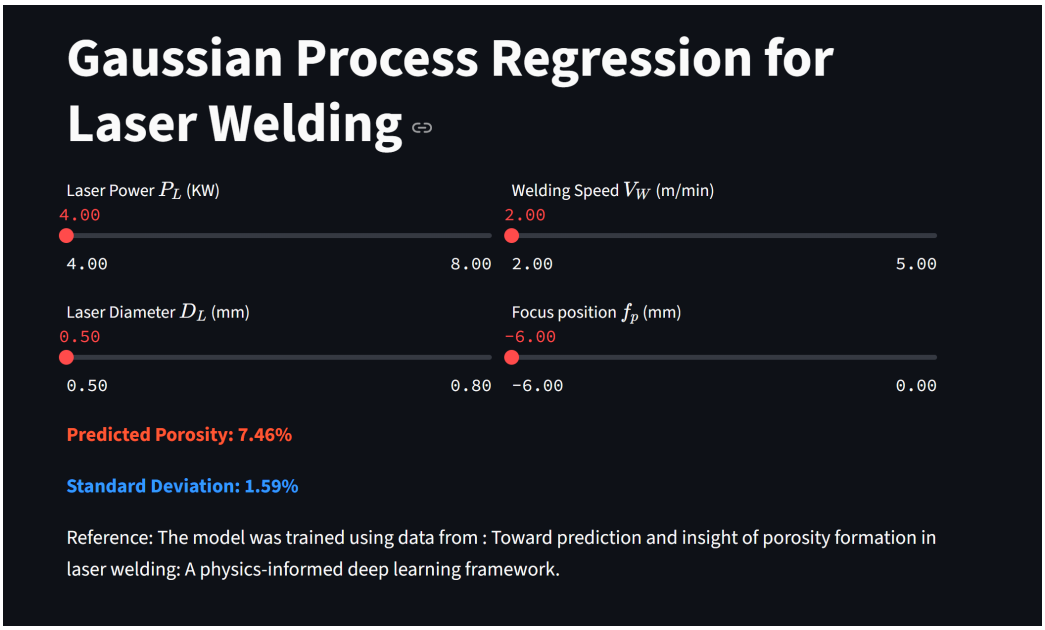

Figure 3 Screenshot of the web-hosted streamlit app based on the extracted GPR model for the laser welding dataset

Gaussian Mixture models for process window identification

In metal AM, Gaussian Mixture Models (GMMs) can serve as powerful tools for process monitoring, defect detection, and microstructural classification. GMMs represent complex, multimodal distributions by combining multiple Gaussian components i.e a GMM assumes the analysed data arises from a weighted sum of Gaussian distributions, each with its own mean and covariance. The Expectation-Maximization (EM) algorithm iteratively estimates component parameters and mixture weights to maximize the likelihood of observed data.

For this ROM demonstrator, the process window identification at the single track scale for laser PBF was selected. The dataset for the analysis, consisting of 166 data points, was extracted from https://ars.els-cdn.com/content/image/1-s2.0-S2352940721001888-mmc1.pdf and was part of a study by Du et al (Du et al 2021) on physics informed ML model development. A preliminary single component model extraction had shown a maximum predictive accuracy of 16% only. This was attributed to the different materials (a categorical variable) included in the dataset, the three modes of defects (lack of fusion, keyhole porosity and humping) being clubbed together and due to the corresponding small size of the dataset for each material.

The GMM implementation involved generating two separate models for likelihood of defect formation and likelihood of process success, with a decision boundary being defined through hyperparameter tuning for when to switch between the two sub-models. A squared

exponential kernel function was chosen for each case and the EM algorithm was used to tune the model fitting parameters for both sub-models. The accuracy of the resultant GMM was over 99%. Figure 4 shows the results of the GMM model for SS 316L on the power vs scan speed parameter space. The red and blue zones correspond to the regions where the log-likelihood of defect formation and the log-likelihood of process success were higher respectively. The plus '**+**' markers denote the training dataset for the sub-model for process defects, while the crosses '**X**' denote the corresponding test dataset. Similarly, the triangle '**🡐**' markers denote the training dataset for the sub-model for process success, while the circles denote the corresponding test dataset.

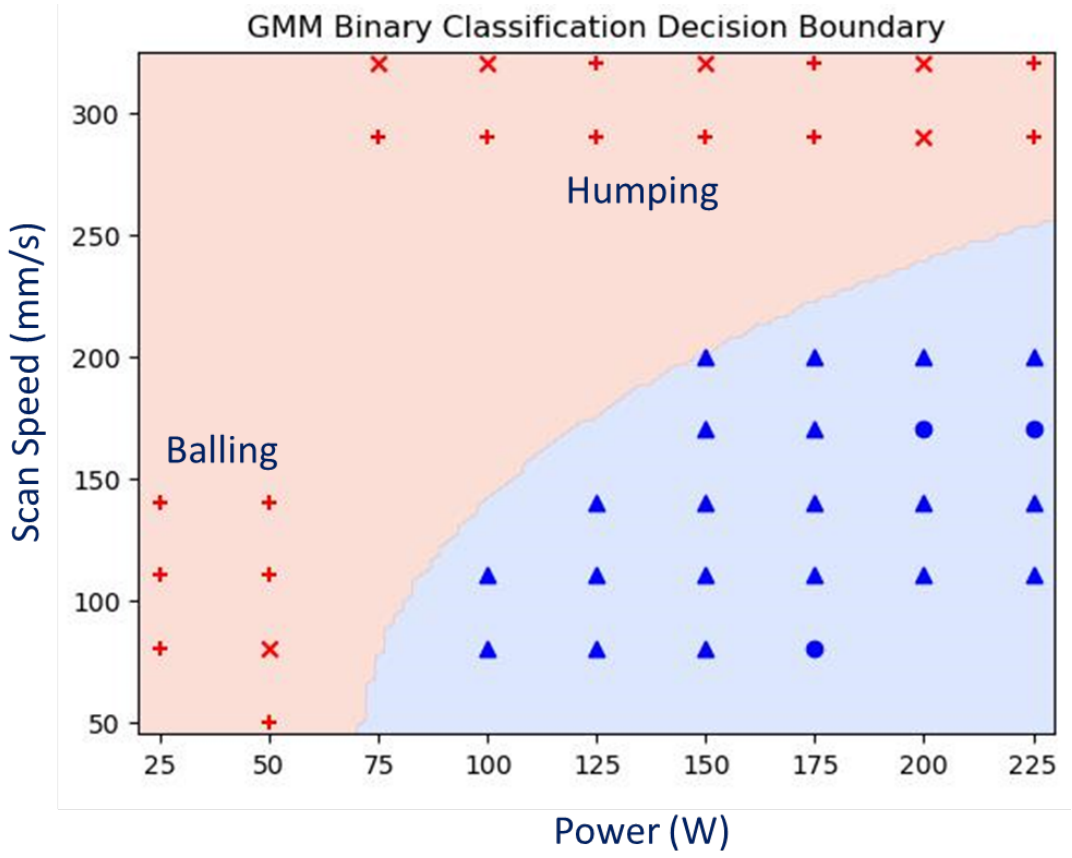

Figure 4 Process parameter space showing the results of the GMM developed in DILAPRO for process window identification

3.2 Deep learning based ROM

Generative AI models for surface topography prediction

This ROM offers a significant advancement in the ability to anticipate and optimize process routes for surface quality in metal AM. In this case, a novel deep learning-based conditional denoising diffusion probabilistic model was established for generating synthetic yet physically

realistic PBF surface topographies. Metal AM specimens were fabricated at DTI and DTU across controlled parameter spaces, and high-resolution 3D surface morphology data was acquired using confocal microscopy. The measured point cloud data was processed into 2D height maps and paired with critical process parameters. The deep learning model, trained on datasets with multiple types of morphology pattern, demonstrated the ability to generate synthetic surfaces through parameter interpolation while maintaining key stochastic features.

The artefacts used for generation of the surface morphology models corresponded to a series of rectangular cuboids of 10mm width and 10.76 mm height, with 400 µm of additional layers printed on its top surface with rhombic patterns as shown in Figure 5. The length of the samples varied from 40 mm to 65 mm, while the included angle in the rhombic pattern varied from 5 deg to 45 deg. The 316L artefacts were manufactured on a SLM280 system without the use of upskin parameters and contour parameters that are typically utilized in industrial production settings. The scan strategy was rotated by 67 degrees every layer for the cuboidal base sample, but no scan rotation was performed for the 400 µm rhombic structure. A parallel scanning pattern was used for the rhombic structure, with the scan lines running parallel to the shorter side of the cuboidal base. The artefacts were fabricated in different steel materials (e.g. 17-4PH and 316L) to also include the material dependence.

In each case, the acquired surface morphology was saved as an image and subsequently subjected to Gaussian blurring:

$$I_\sigma(x,y) = (I * G_\sigma)(x,y) = \iint_{-\infty}^{\infty} I(u,v) \cdot G_\sigma(x-u, y-v)\, du\, dv$$

where the 2D Gaussian kernel is:

$$G_\sigma(x,y) = \frac{1}{2\pi\sigma^2} \exp\left(-\frac{x^2+y^2}{2\sigma^2}\right)$$

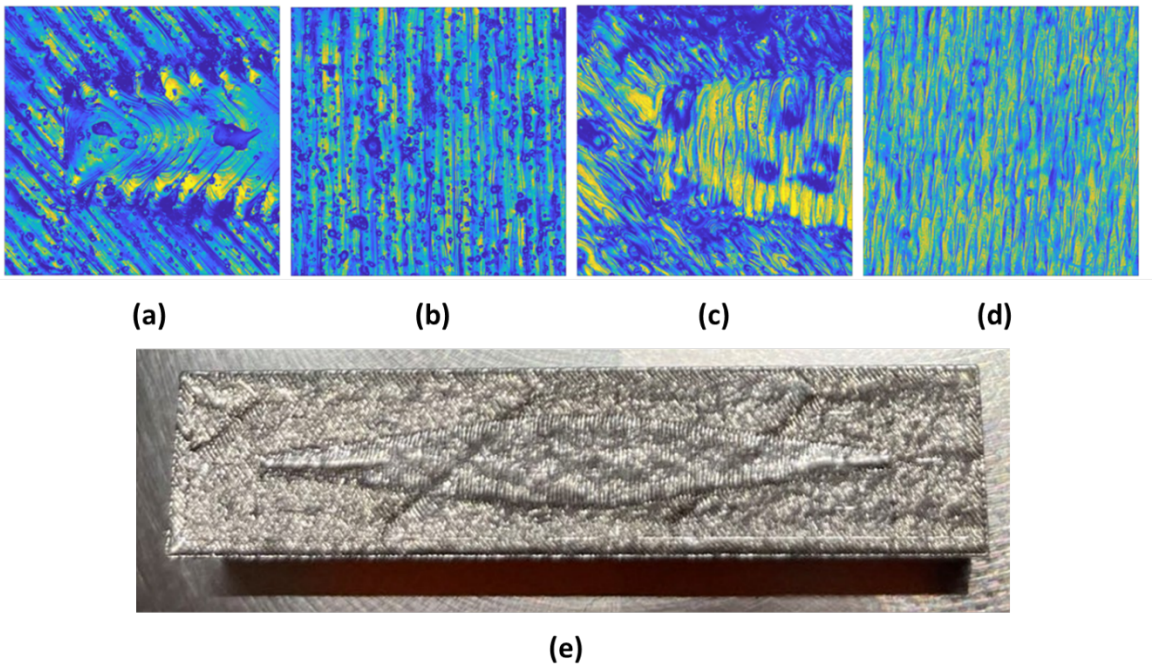

Figure 5 (a)-(d) Optical microscopy images acquired using Olympus LEXT system from different location of the various PBF samples, and (e) one of the produced samples showing the rhombic printed pattern over a printed rectangular block

In addition to the morphological differences between the measured samples, the location of a point—whether it lies within the rhombic region—also influenced the surface morphology. To account for this, a two-dimensional word embedding was used to provide conditional inputs to the deep learning based diffusion model for the surface morphology. Due to the distinct surface morphology within the rhombic region compared to its surroundings, random cropping was performed separately inside and outside the rhombus, yielding 400 images of size 256 X 256 pixels for each region.

The deep learning based ROM consisted of a conditional U-Net backbone for noise prediction and a diffusion process wrapper that implemented the forward noising process. The details of the implementation can be found in the corresponding publication on this topic (Shan et al 2025). Figure 6 shows examples of real and generated surfaces using the deep learning ROM, wherein all images in the first column and all images in the last row are generated surfaces.

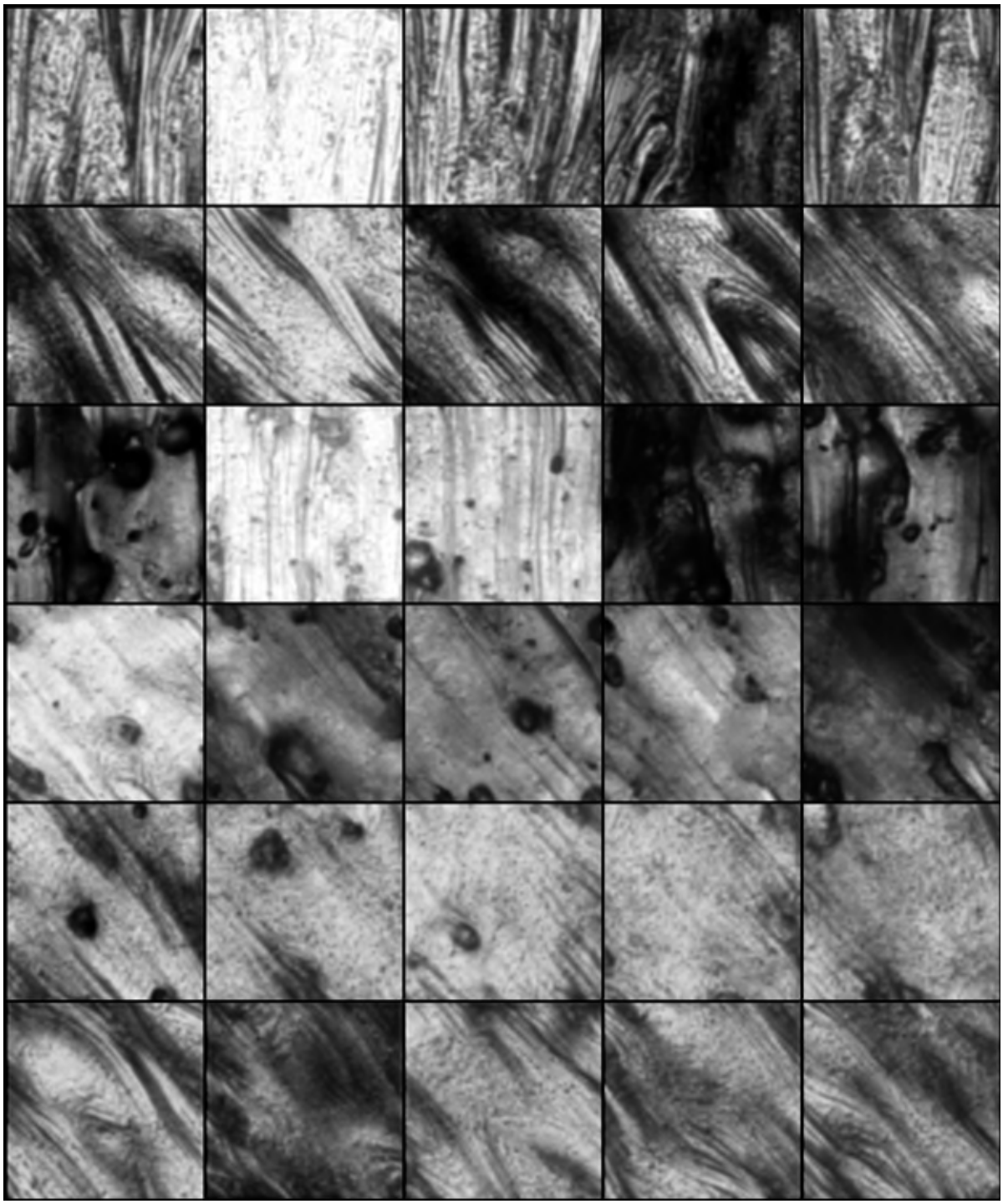

Figure 6 Real and generated surface topographies using the generative AI ROM from DILAPRO.

ML based ROM for advanced image segmentation

Image segmentation is an essential step in modern microscopy and CT analysis, and consequently several ML models are available in literature that focus on this task (as well as on image classification). The image segmentation ROM developed here focuses on low-contrast images (e.g. from optical microscopy, SEM and/or XCT) containing two or more components of interest. The architecture used for the deep learning segmentation task was based on U-Net. In comparison with other architectures, U-Nets have shown excellent performance in image segmentation as the visual information is restored through the encoder-decoder architecture, and they also perform well on smaller datasets. The chosen architecture is further of the type utilising the deep CNN ResNet34 (He et al 2016) as the backbone, where the ResNet34 is pre-trained on the ImageNet dataset (Deng et al 2009).

As demonstrator for this category of models, synchrotron images of AlSi10Mg samples manufactured by PBF (produced at DTI but measured in collaboration with a separate parallel project at DTU) were analyzed to identify Si particles and/or network as well as Fe containing precipitates (e.g. the π-$Al_8Si_6Mg_3Fe$ phase). The dataset for training the deep learning segmentation model (comprising of multiple original high-resolution images) was established by cropping the original dataset into 256 X 256-pixel patches.

Two separate implementations were performed – the first implementation distinguishing between Al and Si (where all other similar contrast objects were classified as Si) and the second implementation wherein Al, Si and Fe-containing phase were segmented. In each case, the loss function used in the training of the U-Net was weighted categorical cross-entropy loss (Ho et al 2020), where the classes {0, 1, 2} were assigned weight {0.0, 1.0, 1.0}, meaning no weight on the areas having no label and equal weight on the labelled areas. The networks were trained using an ADAM optimiser for 200 epochs, showing a convergence of the training and validation losses. The Intersection-over-Union (IoU) metrics was used to track model performance.

$$IoU = \frac{|A \cap B|}{|A \cup B|}$$

where A and B are the segmentation and annotation, respectively.

Figure 7 shows the results for the two-component image segmentation ROM. Example images from the test and training dataset are shown, along with annotated images comparing the segmentation with the manually labelled ground truth. The IOU scores during the training epochs and the convergence of the loss function are also shown, along with the confusion matrices for the training dataset and the test dataset. Figure 8 shows the same results for the

three-component image segmentation ROM. Both models have high precision and acceptable accuracy values.

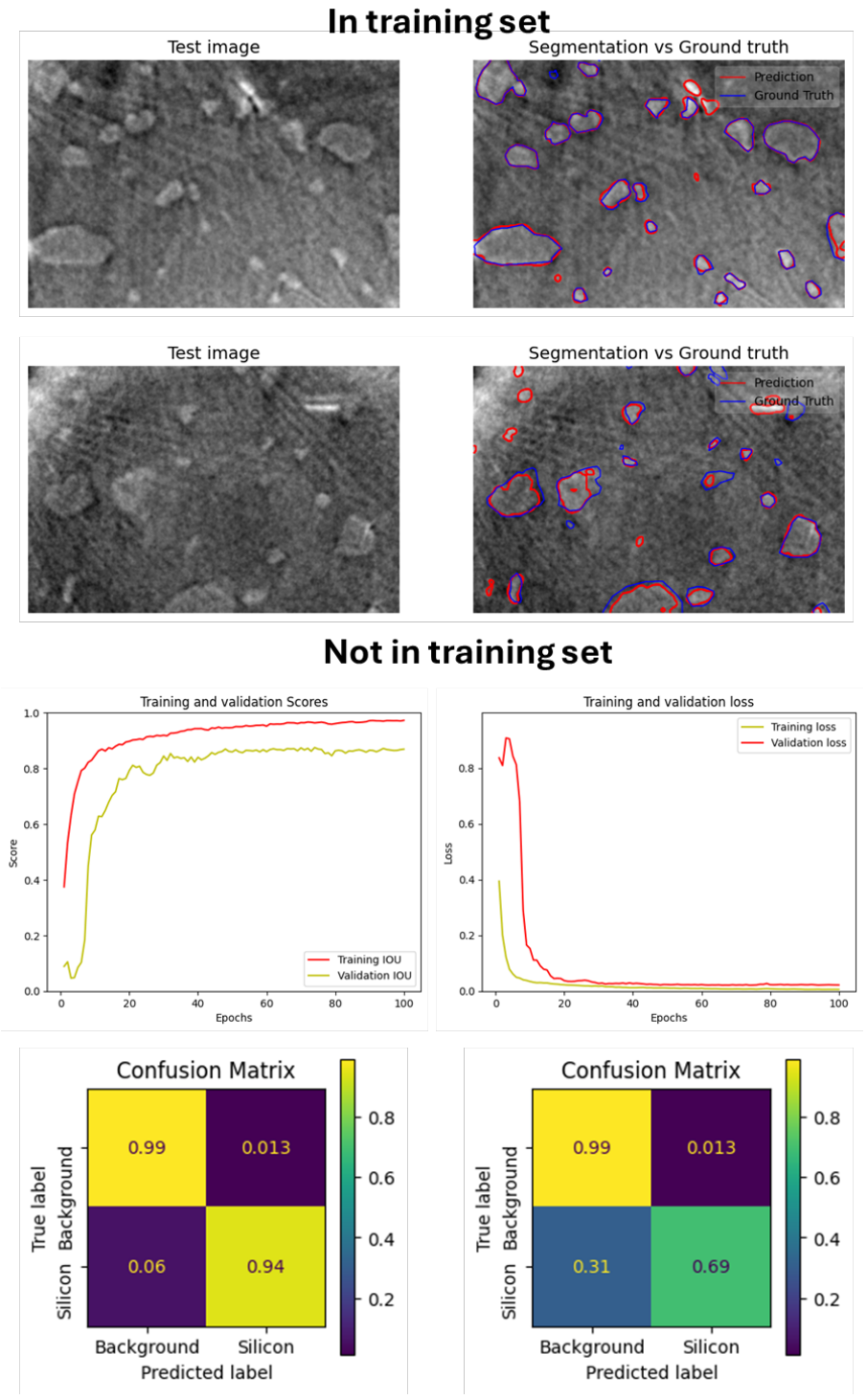

Figure 7 (Top two rows) Training and test image datasets along with corresponding annotated images showing ground truth, (third row) the IoU score and the loss evolution during training epochs, and (bottom row) the confusion matrix for the training (left) and validation (right) image datasets. The model has high precision and acceptable accuracy.

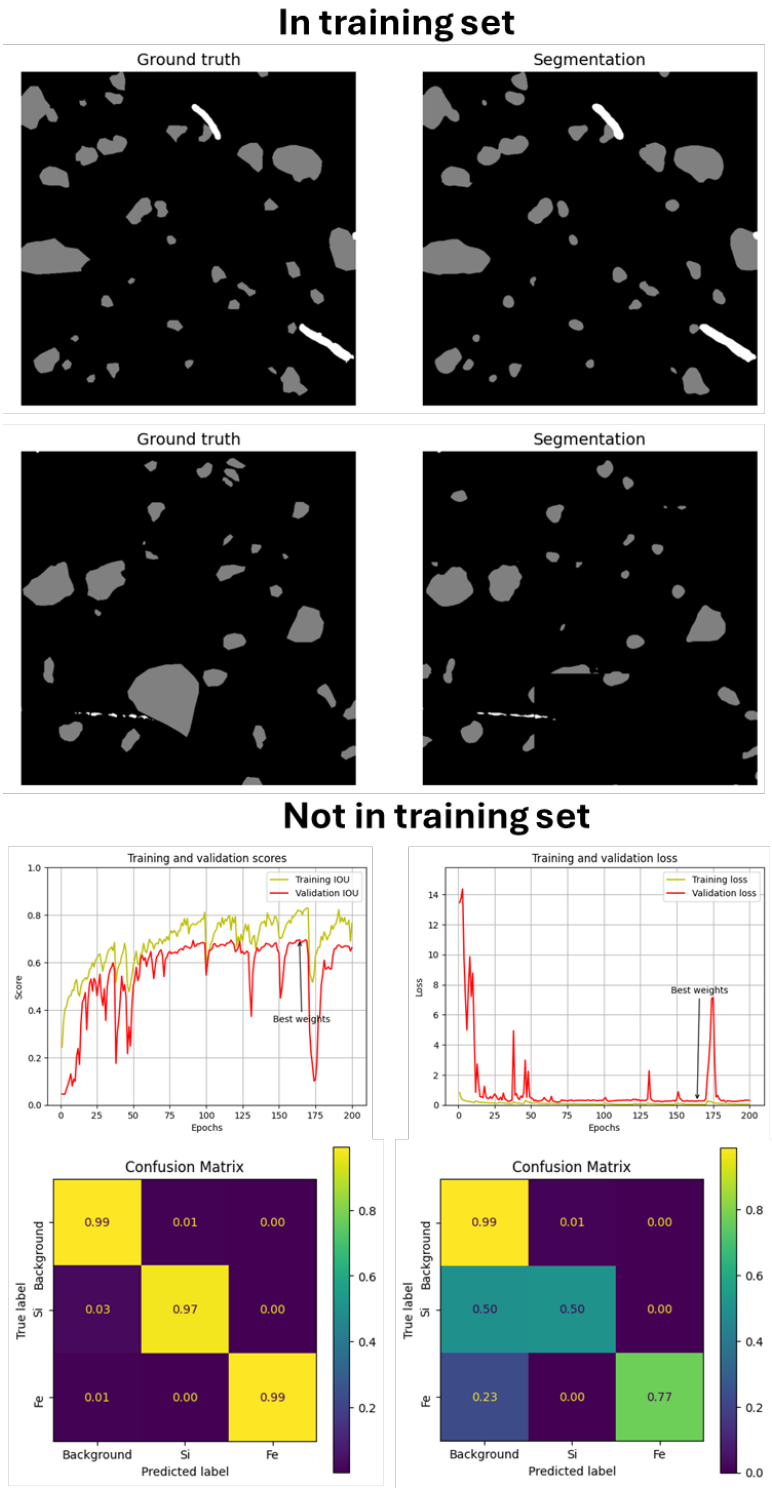

Figure 8 (Top two rows) Training and test image datasets along with corresponding annotated images showing ground truth, (third row) the IoU score and the loss evolution during training epochs, and (bottom row) the confusion matrix for the training (left) and validation dataset. The model has high precision and acceptable accuracy.

3.3 Hybrid ROMs combining data models with simpler simulations

This ROM utilized extensive measurement data to establish correlations between the geometrical measurements of artefacts produced by PBF and the in-process thermal images captured during production. The ROM has the potential to reduce the need for post process quality inspection steps, such as CT scanning.

The workflow involved production of 160 small artefacts of 5mm X 5mm X 5mm dimensions at different locations of the powder bed (as a collaboration with a parallel project on digitalization of manufacturing). The artefact contained multiple small geometrical features that were subsequently measure with optical CT methods. Far-field powder bed temperatures were recorded at 4 different occurrences: after re-powdering, before laser scanning, after laser scanning and before re-powdering. The temperature during the cooling stage is simulated instead using a finite difference model, as the external temperature typically rapidly approach the ambient values while the interior remains at an elevated level. Subsequently, a recurrent neural network, specifically a long short-term memory model was implemented that allowed handling of time-series temperature data. The ML model allowed prediction of the dimensions/quality of the geometrical features based on the combination of the measured thermal data during production and the simulated temperature data during cooling.

Figure 9 shows the artefact design and the measured correlation between the average temperature at a location and the resultant dimension of a geometrical feature (statistical correlations were evaluated for all 29 features in the artefact). Further, in Figure 9, the measured diameter across the build plate can be compared against the predicted diameter from the ROM.

The details of the experimental study and the ROM can be found in the recent article (Calaon et al 2025). The model can be directly implemented when DILAFACT is extended to polymer materials. The developed technique, however, is applicable to the current production lines of DILAPRO as well, where a combination of acoustic, eddy current and thermal sensing methods are being deployed (in WP3). Heatmaps can be generated using any and/or a combination of these sensing methods and the developed ROM can be retrained (via transfer learning) for the specific production lines to account for the correct sensor data.

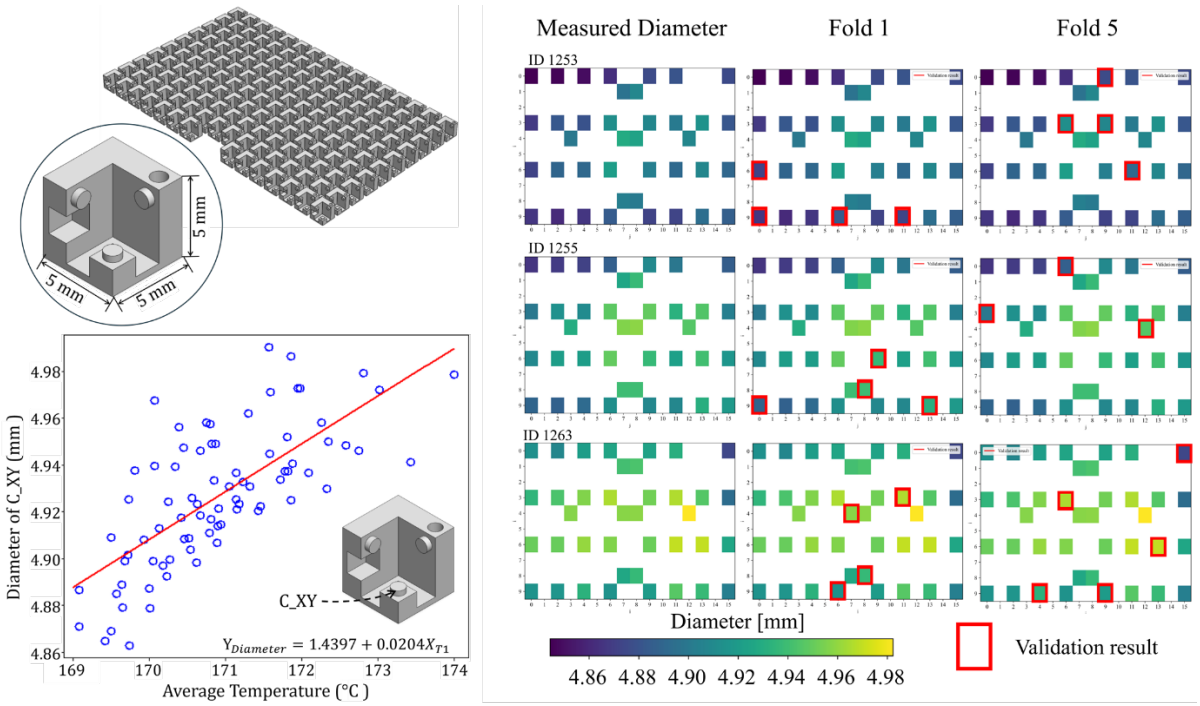

Figure 9 (Top left) Design of the artefact and the build job, (bottom left) Correlation between diameter of a geometrical feature and the estimated average temperature, and (right) the measured and predicted diameter values for all artefact in the build job.

4. Summary and Outlook

This report highlighted different types of reduced order models developed within DILAPRO project. A status update was provided on prior identified modelling tools in D2.1 and activities needed before their implementation in DILAFACT (within WP7). Subsequently new ROMs based on Gaussian Processes and ROMs based on ML techniques were showcased with example results.

Within WP7, the different ROMs will be further improved and fine-tuned for the different production lines and material combinations. The current deliverable has focused on examples of laser additive manufacturing and one example of laser welding, while the experimental campaign and development of ROM for laser texturing is planned within WP7 instead. In addition, expanding the model datasets with experimental results from WP3 and coupling these ROMs to models developed for feedback control and online defect detection within WP3 will potentially increase the predictive accuracy of DILAFACT (an activity planned in WP7).

Bibliography

- Calaon, M., Yeh, H.-P., Shan, S., Hattel, J. H., Zhang, Y., & Hansen, H. N. (2025). Advancing quality prediction in polymer PBF-LB: a hybrid AI and physics-guided approach. Cirp Annals - Manufacturing Technology. https://doi.org/10.1016/j.cirp.2025.04.027
- DILAPRO. Deliverable 2.1: Multi-scale multiphysics simulation framework with hierarchical modelling workflows for selected material. DTU. 2024.
- DILAPRO. Deliverable 2.3: Manual guides for the methodologies of physically simulating the AM process and laser surface interaction. IMDEA. 2025
- DILAPRO. Deliverable 3.3: Report on real-time feedback control algorithm. DCU. 2025
- Deng, J., Dong, W., Socher, R., Li, L.-J., Li, K., & Fei-Fei, L. (2009). ImageNet: A large-scale hierarchical image database. 2009 Ieee Conference on Computer Vision and Pattern Recognition, 248–255. https://doi.org/10.1109/CVPR.2009.5206848
- Du, Y., Mukherjee, T., & DebRoy, T. (2021). Physics-informed machine learning and mechanistic modeling of additive manufacturing to reduce defects. Applied Materials Today, 24, 101123. https://doi.org/10.1016/j.apmt.2021.101123
- He, K., Zhang, X., Ren, S., & Sun, J. (2016). Deep Residual Learning for Image Recognition. 2016 Ieee Conference on Computer Vision and Pattern Recognition (Cvpr), 770–778. https://doi.org/10.1109/CVPR.2016.90
- Ho, Y., & Wookey, S. (2020). The Real-World-Weight Cross-Entropy Loss Function: Modeling the Costs of Mislabeling. Ieee Access, 8, 4806–4813. https://doi.org/10.1109/ACCESS.2019.2962617
- Meng, X., Bachmann, M., Yang, F., & Rethmeier, M. (2025). Toward prediction and insight of porosity formation in laser welding: A physics-informed deep learning framework. Acta Materialia, 286, 120740. https://doi.org/10.1016/j.actamat.2025.120740
- Shan, S., & Mohanty, S. (2025). A Deep Learning Approach for Predicting Surface Topography in Laser Powder Bed Fusion (PBF-LB) Additive Manufacturing. IOP Conference Series: Materials Science and Engineering, NOLAMP20 conference (Accepted)

